JOURNAL OF PROPULSION AND POWER
Vol. 16, No. 6, November–December 2000

Electrical Characteristics of Magnetohydrodynamic-Generator Sidewalls with Segmented Z-Bar Design

Carlson C. P. Pian*
Mississippi State University, Mississippi State, Mississippi 39762
and
Stanley W. Petty†
Textron, Inc., Wilmington, Massachusetts 01887

The electrical characteristics of segmented Z-bar insulator walls for magnetohydrodynamic power generators have been investigated. Experiments were carried out, using a 20-MW (thermal input) power generator, to compare the performance of the Z-bar sidewall design to that of the conventional straight-bar configuration. Electrical properties were measured for clean-fuel (bare-wall) and simulated coal-fired (slagged-wall) test conditions. The Z-bar sidewall design was found to be superior for its ability to adjust to varying generator load and operating conditions. The wear-inducing electrical stresses were much lower and more uniformly distributed in the Z-shaped configuration than in the straight-bar design. The effects of bar segmentation on the interbar voltage and fault power distributions were also studied. The selection of sidewall design for several recent power generators was based in part on the results of this study.

Nomenclature

$\boldsymbol{E}$	=	electric field intensity, V/m
E_x	=	axial electric field intensity, V/m
E_y	=	Faraday field intensity, V/m
E_{yc}	=	value of E_y in the core flow region, V/m
I_e	=	electrode current, A
I_{sc}	=	interbar short-circuit current, A
N_{ovlp}	=	number of overlapped electrodes
V_{Hall}	=	Hall voltage of generator, V

I. Introduction

THE rectangular cross-sectioned flow channel of the magnetohydrodynamic (MHD) power generator is formed by four walls. The two walls having surfaces parallel to the magnetic field vector are the electrode walls. The sidewalls separating the electrode walls are insulator walls. Because of the unavailability of electrical insulating materials that can reliably withstand the harsh environment inside coal-fired generator channels, the insulator walls are typically constructed of water-cooled metal elements that are insulated from each other to prevent any net flow of current.[1] Figure 1 shows several typical insulator wall designs.

Figure 1a shows a peg wall design. These walls are constructed of rectangular or square metallic elements (pegs), typically 2–3 cm on a side, separated by thin strips of insulator material. The advantage of this design is its electrical flexibility and its superior electrical insulating properties under all kinds of generator operating conditions. The disadvantages are the mechanical complexity arising from the large number of small elements and the need for internal manifolding within each row of pegs for cooling. With proper engineering and assembly procedures, such walls can be made to operate reliably and have, in fact, been tested at the 20-MW (thermal input) generator size for hundreds of hours. Scaling of the peg wall to large commercial sizes is difficult because of the large number of wall elements.

Received 10 April 1999; revision received 13 December 1999; accepted for publication 20 December 1999.

*Professor, Research, Diagnostic Instrumentation and Analysis Laboratory; formerly, Textron Everett Research Laboratory, Everett, MA 02144. Associate Fellow AIAA.

†Principal Research Engineer, Energy Technology Office, Systems Division, retired.

To simplify insulator wall design, the conducting-bar sidewall, shown in Fig. 1b, is used. The sidebar elements lie nominally along the direction of equipotential planes in the generator. The sidebars also serve as the diagonal connections for electrode currents to flow from the cathodes to the anodes. This design is hydraulically more reliable than the peg design, having no internal manifolding of coolant. Such continuous-bar design however can only be used in diagonally-loaded generators and it does not allow external current control or fault power control.

To alleviate these problems, the conducting sidebars are split, as shown in Fig. 1c, which allow the use of external circuits for electrode current control. Each sidebar segment is large enough to be individually cooled. In comparison to the continuous sidebar design already discussed, the segmented bar design requires a larger number of coolant hoses and penetrations of the pressure vessel.

A disadvantage of the bar-style sidewall designs is their inability to follow changing potential distribution in the plasma. When the bar orientation becomes misaligned with the plasma equipotential plane, sidebar elements span voltage gradients that can cause circulating currents to pass between the sidebars and the plasma, as well as current leakage and arcing between the bars. Misalignment can occur in the electrode boundary-layer regions of the channel or when the generator is operated at off-design conditions.

Segmented-bar sidewall designs have been extensively tested in both oil- and coal-fired MHD generators. Material wear due to interbar current leakage and arcing have been observed. The locations of the wear on the sidewalls of a 50-MW (thermal input) coal-fired generator are shown in Fig. 2. Material loss occurred at the upstream edges of the long cathode sidebars near where these bars overlap the upstream midbars. The wear patterns suggest anodic erosion due to leakage currents and/or arc discharges. These wear locations corresponded to positions where high interbar voltages were measured.[2,3] Anodic protection, using brazed tungsten and tungsten–copper surface caps, has been tried on the cathode sidebars with varying degrees of success.

The other wear areas, at the corners where the anode wall joints the sidewalls, also coincided with locations where high insulator-gap voltages were measured. Anode material losses from arc melting were observed during posttest inspections. The direction of the arc current is from an anode to its upstream anode sidebar. In most cases the wall corner joint insulating seal is punctured by arcs, whereas the interanode insulators remain intact.

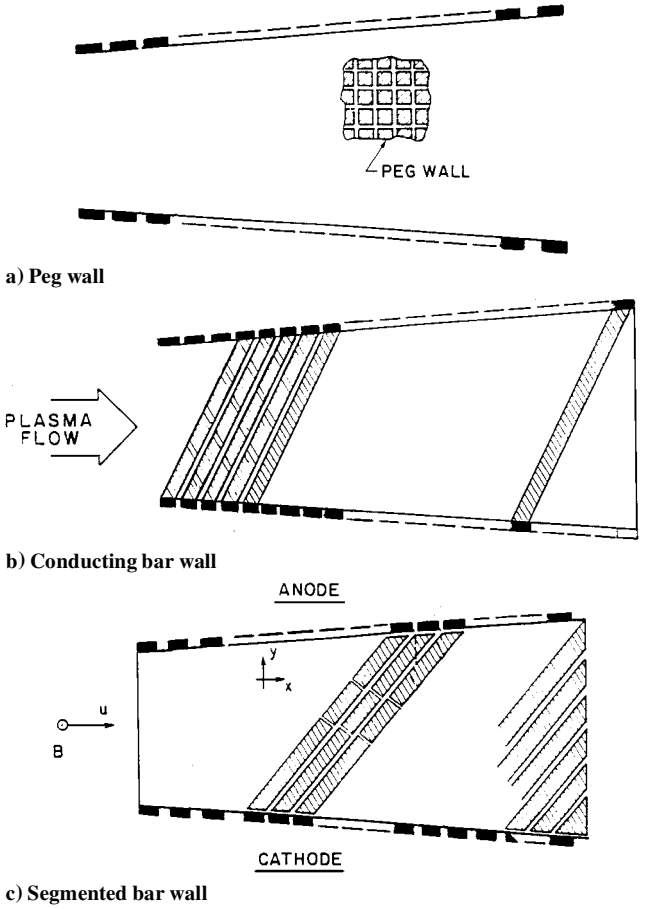

Fig. 1 Insulator sidewall designs.

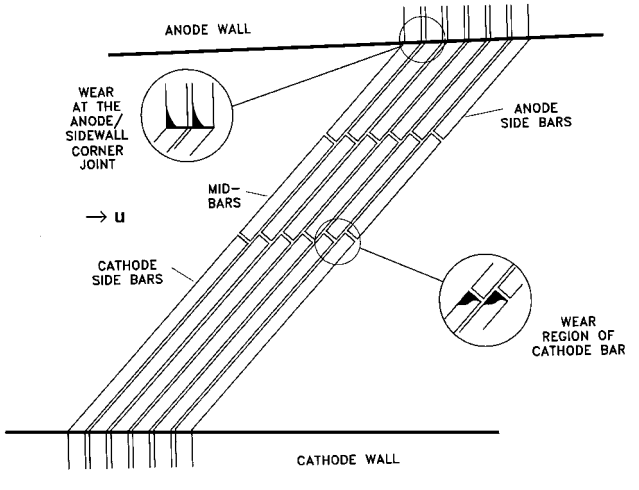

Fig. 2 Observed wear patterns on the sidewalls of a 50-MW coal-fired generator channel.

A variation of the segmented-sidebar design is the Z-bar design, shown in Fig. 3, in which the wall elements are arranged to follow more closely the actual shape of equipotential planes in the generator. The heights of the two vertical elements within the Z-shaped rows are selected to approximate the thickness of electrode wall boundary layers. Such a design was selected for a recent coal-fired, proof-of-concept MHD generator.[1,4]

This paper describes MHD generator tests carried out to study the electrical properties of segmented Z-bar sidewalls. The effects of cathode voltage nonuniformities and sidebar segmentation on the wear-inducing electrical stresses were also investigated. The descriptions of the sidewall tests are presented in Sec. II. The generator channel used in the tests was assembled so that one of the sidewalls has the Z-bar wall design, while the other has the conventional straight-bar design. This arrangement allowed one to compare directly the performance of these two types of sidewall designs under similar test conditions. Results from clean-fuel generator tests are reported in Sec. III, whereas those for slagged-wall tests are described in Sec. IV.

Table 1 Generator operating conditions and channel geometry of sidewall comparison tests

Parameter	Value
Total mass flux, kg/s	2.0
Oxidant N/O ratio	0.7–0.8
Seed fraction, wt% potassium	1.0–1.5
Oxygen stoichiometry	0.9
Equivalent ash carryover, %	0 and 30
Peak magnetic field intensity, T	2.5
Generator channel length, m	1.0
Channel height, m	
Inlet	0.15
Outlet	0.18
Channel width, m	
Inlet	0.07
Outlet	0.12

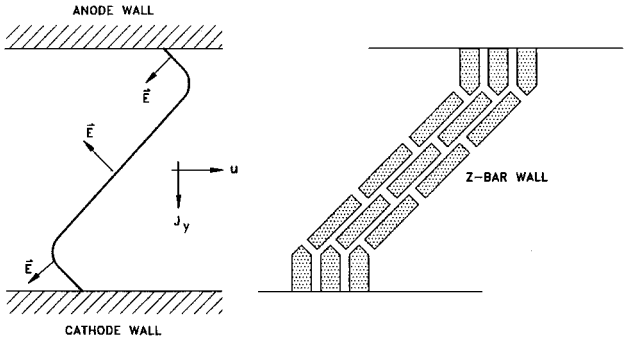

Fig. 3 Z-bar insulator wall design.

II. Mk-VII Insulator Sidewall Tests

The sidewall tests were carried out in the Mk-VII MHD facility, a 20-MW (thermal input), 3-T test facility, using a workhorse generator channel. The plasma source was an ash-injected oil combustor, operating with number 2 fuel oil and oxygen-enriched air. Fly ash from Rosebud coal was injected into the combustor to simulate slag carryover. A supersonic channel having an inlet Mach number of 1.2 was used for the tests. This channel was 1.0 m long, consisting of 56 segmented electrode pairs. The generator was diagonally loaded, with external diagonal connections of nine overlapping electrodes (the angle between the diagonal link connection and the vertical plane was approximately 43 deg). Current control devices were used in the external diagonal connections.

Electrodes of the workhorse generator were constructed of copper with stainless steel, platinum, or tungsten caps brazed to the gas-side surfaces. Interelectrode insulators were made of 2.5-mm-thick boron nitride wafers.

Layouts of the two insulator sidewalls are shown in Fig. 4. The right sidewall was configured with straight bars, while the left wall had the Z configuration. Arrangements were made to accommodate two different bar segmentation patterns, consisting of three- and four-segment bar rows, on each of the sidewalls. The nomenclature adopted for the different bar elements within a row of diagonal bars is included in Fig. 4. The sidebars were constructed of copper; insulators were fabricated from strips of boron nitride.

The test conditions and channel geometry are summarized in Table 1. Measurements of the electrical power output, Faraday and interelectrode voltages, electrode currents, and sidewall electrical properties were taken at the various test conditions. The sidebars

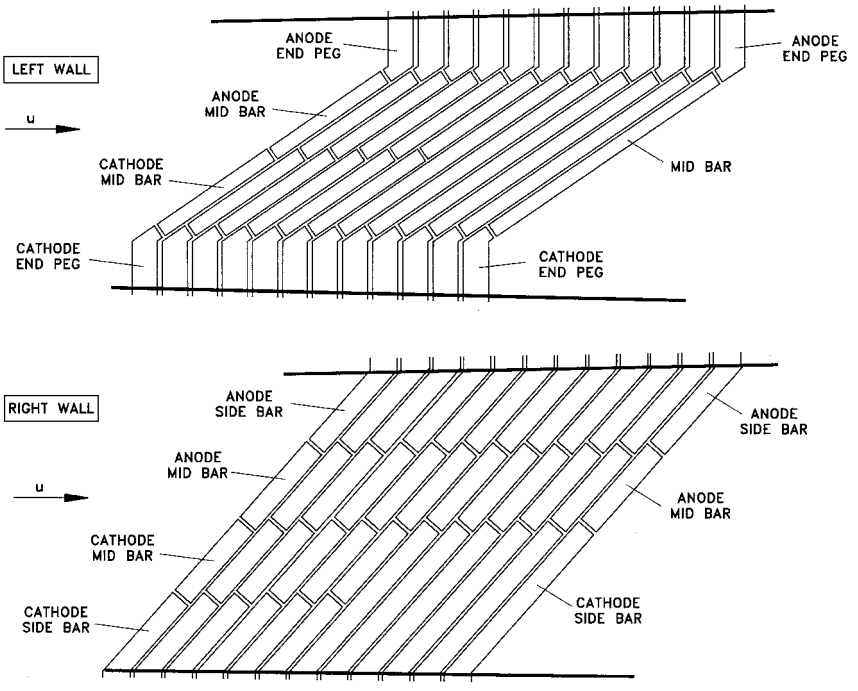

Fig. 4 Layouts of the sidewalls for the Mk-VII bar-wall comparison tests.

on both sidewalls were instrumented to measure the interbar voltages. External switching circuits were also connected to the sidewall elements for measuring the interbar short-circuit currents and for use to obtain alternative sidewall configurations by intentionally shorting out shorter bar elements.

The sidewall comparison tests were carried out for both ash-injected (slagged-wall) and clean-fueled (bare-wall) generator operating conditions. Although bare-wall surface conditions are not representative of coal-fired generator operation, they are included in the present tests because the results provide qualitative performance trends that apply to all sidewall surface conditions, including slagging walls. The bare-wall test data were also easier to measure and to interpret. The voltage and current measurements from the slagging tests were often unsteady and difficult to reproduce due to changing conditions of the slag coverage. Also, the appearance of slag-induced cathode voltage nonuniformities resulted in voltage maldistributions that complicate sidewall performance comparisons.

III. Bare-Wall Comparison Test Results

Using the measured Faraday and interanode voltages, one can make a quick assessment of how well the diagonal-bar orientations are aligned with the plasma equipotential planes under nominal Mk-VII test conditions. As discussed earlier, the amount of sidebar wear that one can expect during extended generator operation is directly related to this misalignment. The streamwise distributions of the measured plasma equipotential angles are compared with the bar-inclination angles in Fig. 5. All angles are measured from the vertical direction. The external and core flow equipotential angles are defined as $\tan^{-1}(E_y/E_x)$ and $\tan^{-1}(E_{yc}/E_x)$, respectively. The external angles refer to the orientation as viewed from outside of the channel (from one electrode wall to another). The values of E_y are determined from the measured Faraday voltages; the values of E_x are estimated from the interanode voltage measurements. The core angles are those in the core region of the duct flow (excluding the boundary-layer regions). The values of Faraday field intensity in the core region, E_{yc}, were inferred from transverse voltage measurements (using a peg-style sidewall) taken during subsequent workhorse generator test operation at similar test conditions. The diagonal-bar rows for both sidewall designs were inclined at an angle that spanned (overlapped) 9 electrodes. The resulting angle

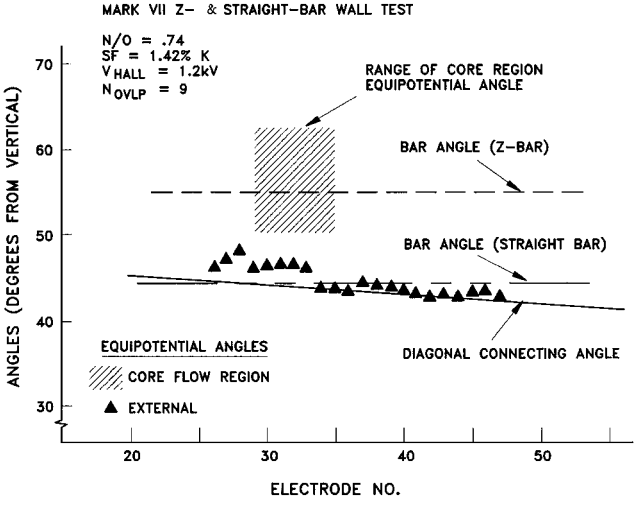

Fig. 5 Equipotential vs sidewall-bar angles, Mk-VII workhorse channel tests.

between the straight bars and vertical was approximately 45 deg, whereas the slanted portions of the Z-bar rows, that is, the two center bars, were about 55 deg from vertical. Figure 5 shows that the orientation of the Z bars generally matches the plasma equipotential distributions, both in the core flow region and near the electrode walls. Misalignment of the straight bars with the gas equipotential, however, is about 10 deg in the core flow region.

Distributions of the electrical parameters as a function of sidebar configurations and segmentation patterns were investigated. Figure 6 shows the various sidewall configurations that were studied during the bare-wall tests. Configurations A and B were the four- and three-segment Z-bar designs; D and E were the straight-bar designs. Configurations C, F, and G were obtained by shorting the anode endbars (or end pegs) to the anode midbars of configurations A, D, and E, respectively.

The interbar voltage measurements for the different sidewall configurations are compared in Fig. 7 at the nominal Mk-VII operating condition. The voltages shown in Fig. 7 are those across the

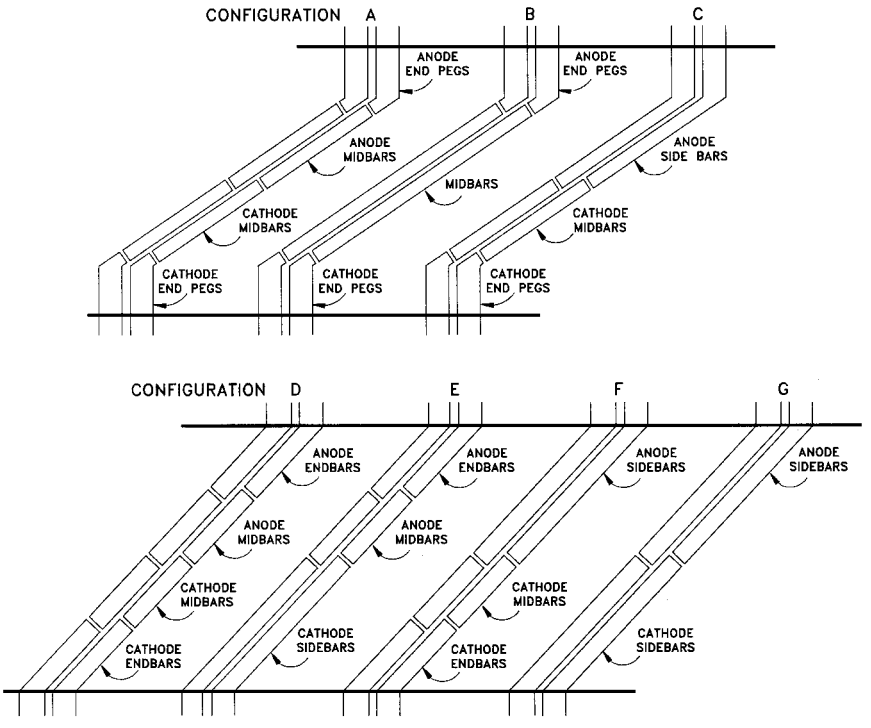

Fig. 6 Sidewall configurations; Mk-VII sidewall comparison tests.

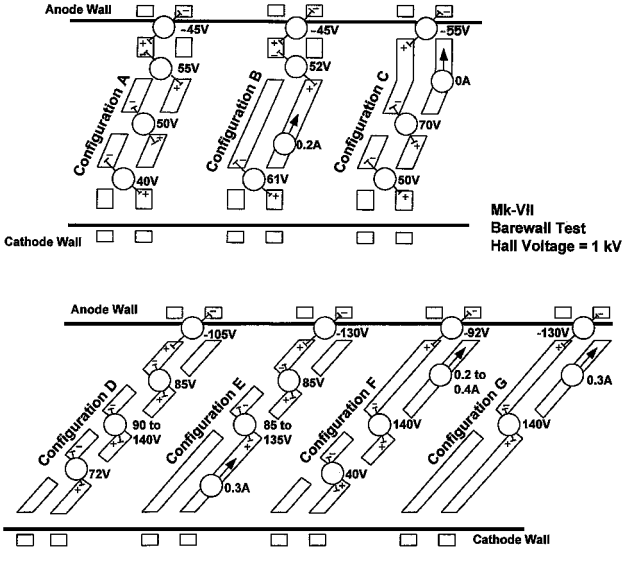

Fig. 7 Measured interbar voltage and inner-bar current distributions; Mk-VII sidewall comparison tests.

anode sidebar-to-downstream anode gaps and the gap voltages in the region of the overlapping midbars, that is, cathode sidebar-to-upstream midbar gap, cathode midbar-to-upstream anode midbar, etc. We compared these particular voltages because material wear was often observed at these locations on the straight-bar sidewalls (see Fig. 2). Results show that the maximum voltages across these critical gaps can be reduced by utilizing a Z-bar configuration and by increasing the bar segmentation. Reduction in the magnitudes of these high voltages decreases the potential for interbar arcing and diminishes the driving force for electrochemical corrosion.

The magnitudes and directions of the bar currents for several selected sidebars are also shown in Fig. 7. These are the currents that exist within the sidebars under nominal Mk-VII generator operating conditions. The driving force for these currents is the voltage gradient set up across the individual sidebars by the generator plasma. The currents exit the sidebars at the upper edges of the metallic elements, causing anodic wear at these locations. The paths of these currents lead to an adjacent sidebar or recirculate to the generator plasma. The greater the mismatch between the sidebar inclination and the plasma equipotential plane is, the larger the magnitude of recirculating current and greater the sidebar wear. The magnitudes of the bar currents were determined by measuring the appropriate interbar shorting currents. For example, the bar currents in the long midbars of configuration B were determined by shorting the anode and cathode midbars of configuration A and measuring the resulting shorting currents. Similarly, the bar currents in the anode sidebars of configuration G were determined by shorting the anode sidebars and midbars of configuration E. Although only a few of these internal bar current measurements were made during the tests, and they were further limited to the long sidebars, the results of Fig. 7 showed that the currents circulating in Z-bar elements were lower than those in the straight bars. The bar currents in the long Z-bar elements were all less than 0.2 A, whereas those in the long straight bars were all over 0.2 A. This trend implies there will be less wear on the anodic edges of sidebars of the Z-bar sidewalls.

Another important parameter to consider in the sidewall comparison is the interbar fault power. These faults result from arcing between adjacent sidebars, or between sidebars and electrode elements, that lead to complete breakdown of the interbar insulator gap. This increases the wear at the corner edges of the affected sidebars and can result in rapid destruction of the interbar insulator. The effects of interbar faults are minimized by limiting the power that can be coupled into such faults. The interbar fault power depends not only on the gap voltage, but also on the rigidity with which the plasma tends to impose such voltages between adjacent bar elements. The fault power is proportional to the product of interbar short-circuit current I_{sc} and open-circuit voltage. The measured interbar I_{sc} for different sidewall configurations are compared in Fig. 8. For the straight-bar sidewalls, the magnitudes of I_{sc} were very high across the gaps between the anodes and their upstream-anode endbar gaps (more than three times higher than for the Z-bar configuration). I_{sc} across the gaps between the cathode sidebars and their upstream-anode sidebars were also large for sidewalls having long cathode sidebars, that is, configurations E and G. The interbar gaps with large short-circuit currents also have very high interbar

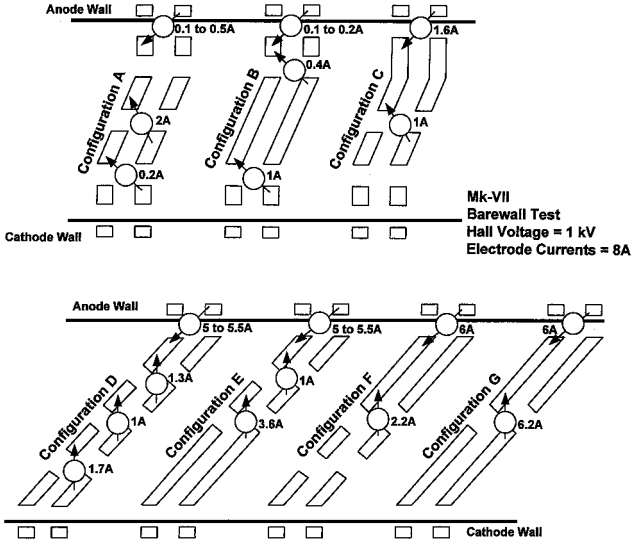

Fig. 8 Measured interbar short-circuit currents; Mk-VII sidewall comparison tests.

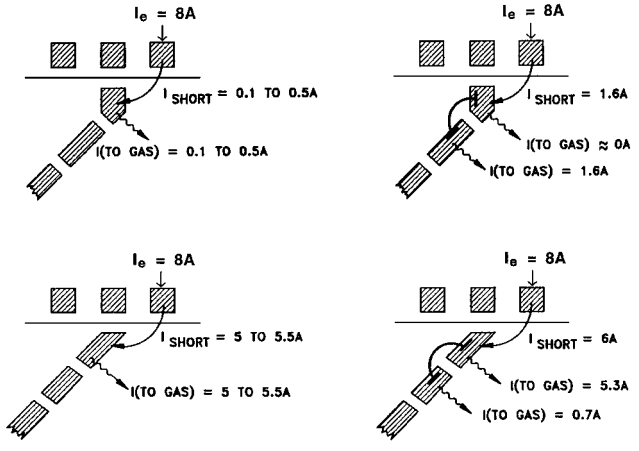

Fig. 9 Comparisons of shorting currents in the anode/sidewall corner regions; Mk-VII sidewall comparison tests.

voltages, as shown earlier in Fig. 7. The combination of large interbar short-circuit current and high gap voltage implies large fault power can be coupled into the interbar arcs, increasing the chances for damaging the sidebar elements. The locations of these gaps are precisely where the greatest material wear was observed on the coal-fired generator sidewalls (shown earlier in Fig. 2).

Figure 9 compares the measured interbar I_{sc} for the various sidebar configurations in the anode/sidewall corner regions and shows the directions and the paths of these currents. The notation of the sidebar configurations refers to that in Fig. 6. Several interesting trends can be noted: 1) The measured I_{sc} and the resulting values of fault power are substantially lower for the Z-bar configurations (configurations A and C) than for the straight-bar designs (configurations D and F). 2) Magnitudes of I_{sc} increased at least threefold when the length of the anode endbar is increased (compare configuration A vs configuration C). This also resulted in a more than threefold increase in the magnitude of interbar fault power. A sidewall arrangement similar to configuration C had been previously considered for a prototypic coal-fired MHD generator design.[4] The longer anode bars would reduce the total number of required sidewall elements and simplify wall construction. However, as a consequence of the present test results, configuration C was eliminated from consideration because of its undesirable fault-power characteristics. 3) The paths taken by the anode-to-sidebar shorting currents are different for the long Z- and straight-bar configurations (comparing configurations C and F). In configuration F, a large fraction of the shorting current (approximately 5.3 A) passes from the anode sidebar and into the gas at a location very near the anode wall, in the boundary-layer region. By contrast, all of the shorting current in configuration C (approximately 1.6 A) enters to the gas at a location much farther away from the anode wall, closer to the core flow region of the channel. In general, current moves from the sidebar to the gas at the location where the voltage gradient between the sidewall and the gas is the greatest. The fact that very little current passes out of the endbars in the anode wall boundary-layer regions (in configurations A and C) suggests that the Z bars are very well matched to the plasma equipotential planes in these wall regions.

IV. Slagged-Wall Comparison Test Results

Voltage nonuniformities occur over the cathode wall of MHD channels operating with slag-laden flows. The influence of these voltage nonuniformities on the electrical performances of segmented-bar sidewalls was investigated in our slagged-wall tests.

Voltage nonuniformities arise when groups of adjacent cathodes are shorted by polarized slag.[5] The polarization of the slag is thought to arise from the ionic nature of current transport across the slag layer, causing deposition of metallic potassium at the electrode surface.[5,6] As a result of these slag-induced shortings, the generator Hall voltage is sustained by just a few nonshorted intercathode gaps. The voltages across these open cathode gaps are substantially higher than when no slag shorting occurs. At times these high gap voltages can exceed 120 V. Typical streamwise and time variations of intercathode voltages from the Mk-VII tests are shown in Fig. 10. Slag shortings on the cathode wall cause electrical potential maldistributions in the plasma, which in turn locally increase the interbar voltages on the sidewalls. Sidebar damages caused by high interbar voltages have been observed.[2,3]

The effects of the cathode nonuniformities on the distribution of interbar voltages for different sidewall configurations are shown in Figs. 11–13. Schematic diagrams showing the measured interbar

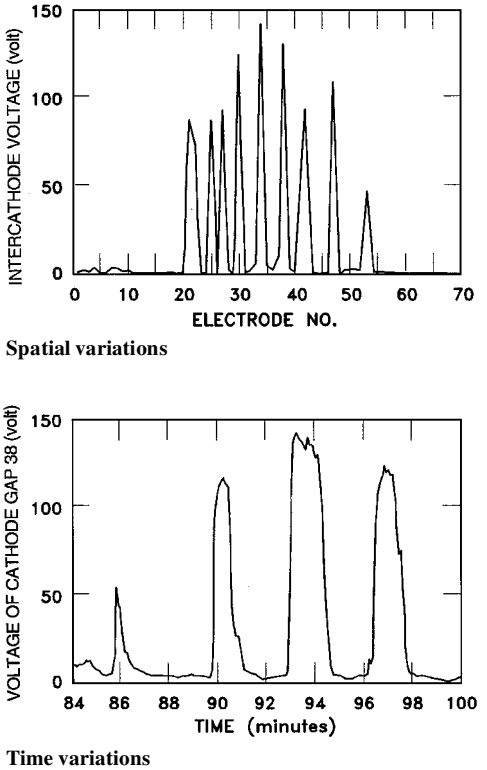

Spatial variations

Time variations

Fig. 10 Typical streamwise and time variations of the intercathode gap voltage.

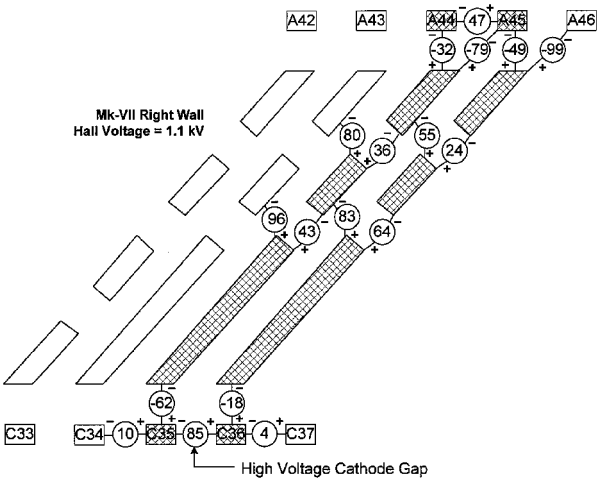

Fig. 11 Interbar voltage distribution when a high-voltage cathode cap is adjacent to the three-segment straight bars.

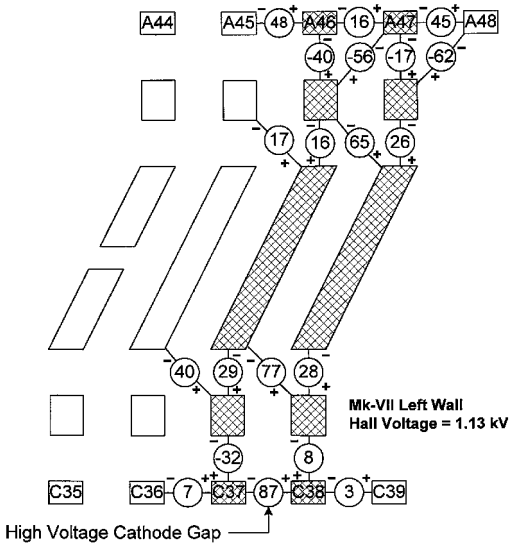

Fig. 12 Interbar voltage distribution when a high-voltage cathode gap is adjacent to the three-segment Z bars.

voltages for the three-segment straight- and Z-bar configurations are shown in Figs. 11 and 12. Figure 13 shows results for the four-segment Z-bar configuration. Because of the transient nature of the voltage nonuniformities, voltage data must be selected from different times during the generator test to compare the various sidebar configurations on an equal basis. Results shown in Figs. 11–13 were taken from those times when a high-voltage cathode gap (approximately 85 V) was situated adjacent to a group of sidebars of interest. Also, the magnitudes of the generator load voltage were all selected to be about the same (approximately 1.1 kV). The measured interbar voltages around the diagonal-bar rows situated immediately upstream and downstream of the high-voltage cathode gaps (shaded bar rows in Figs. 11–13) can be compared between the different sidewall configurations. The Z-bar configuration has lower interbar voltages than the straight-bar configuration under the same stress, that is, a high-voltage cathode gap. The results also show that the influences of the cathode nonuniformities up the sidewalls can be distributed more evenly by increasing the sidebar segmentation.

The comparison was carried out using typical data selected from specific time periods during the slagged-wall test. The same conclusions about sidewall performances can be reached by examining data over the duration of the test. Histograms of interbar voltages

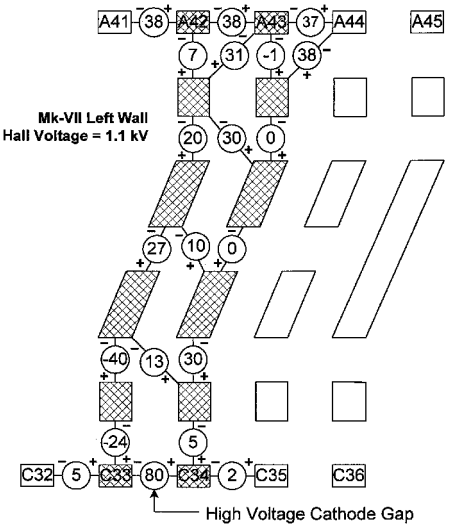

Fig. 13 Interbar voltage distribution when a high-voltage cathode gap is adjacent to the four-segment Z bars.

have been used to determine where the high gap voltages were located, as well as the frequency of their occurrence.[3] The results showed interbar voltages for the straight-bar configurations were very high for a substantial portion of the test. The magnitudes of the cathode sidebar-to-upstream midbar gap voltages (80–100 V) were comparable to those previously measured on the 50-MW coal-fired generator sidewalls.[2] The interbar voltages for the Z-bar sidewall were lower (5–40 V) and much more evenly distributed, especially for the four-segment Z-bar configuration.

Surface protections against erosion and corrosion are required for the sidewall elements of long-duration MHD generators. The designs and material selections of these gas-side cappings are determined from results of duration and engineering testing. As discussed earlier, the range of influence of the cathode nonuniformities is a function of the particular sidewall configuration. The extent of wall regions that require surface protection is determined by how far up the sidewalls that these effects are felt. An example showing the decreasing influence of cathode nonuniformities along the Z-bar sidewall is shown in Fig. 14. Here, the ratios of gap voltage to intercathode voltage are compared for different interbar gaps in the vicinity of the cathode wall. The ranges in the values of the voltage ratio are due to variations in the slagging test data. Results of Fig. 14 indicate that the influences of voltage nonuniformities are weak beyond two horizontal rows above the cathode wall. The magnitudes of the voltage signature at these locations have been reduced to less than 25–30% of those of the source voltages (the high intercathode voltages). The sidebar capping strategy for a recent prototypic MHD generator was based on these test results.[4] To simplify the construction of these Z-bar sidewalls, only two horizontal rows of bars nearest to the cathode wall were fabricated with tungsten caps; the remaining four rows of sidebars were uncapped.

The tradeoffs between bar segmentation and surface capping requirements must be considered to simplify sidewall construction. Sidewall designs with coarse bar segmentation will require fewer numbers of total sidebar elements. However, for sidewall designs with long cathode sidebars, such as those of Figs. 2 and 8, high interbar voltages can appear halfway up the sidewalls. Hence, complicated protective cappings may be required for large fraction of the sidewall surfaces. The influences of the cathode nonuniformities can be attenuated more quickly through greater segmentation of the cathode sidebars. Greater number to sidebars will then have to be fabricated for each sidewall. However, only sidebars situated near the cathode wall will require surface cappings. The majority of sidebars on each sidewall can be of the simpler uncapped design. One must strike a balance between the complication of fabricating many small sidebar elements vs the complexity of incorporating cappings over large portion of the sidewalls.

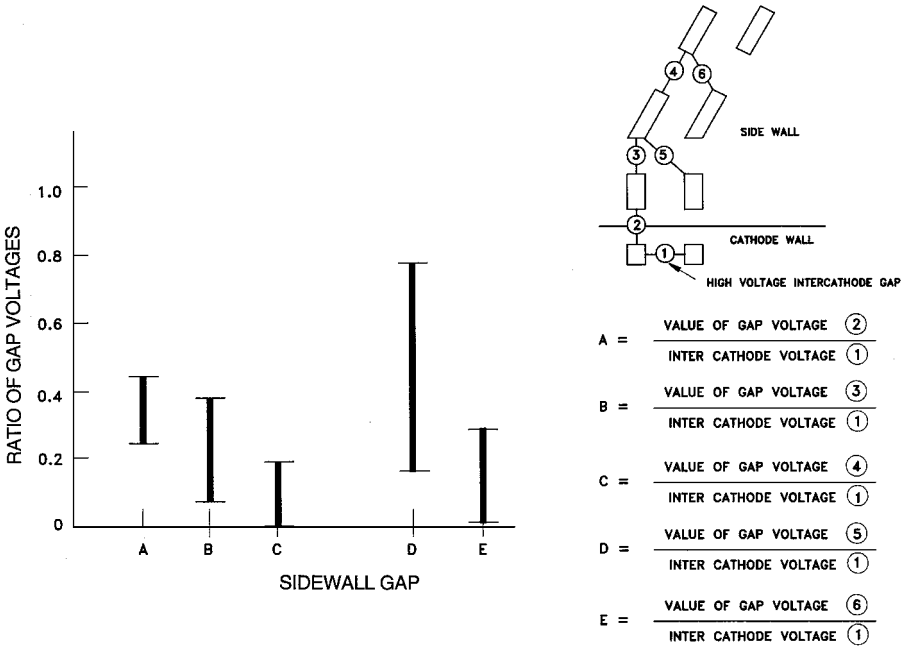

Fig. 14 Decreasing influence of the high cathode-gap voltage along the sidewall.

V. Conclusions

MHD power generator experiments were carried out to study the electrical characteristics of segmented Z-bar insulator walls. Analysis of the test data, for both slagging- and bare-wall operating conditions, showed that the wear-inducing electrical stresses were lower and more evenly distributed for the Z-shaped configuration than in a conventional straight-bar design. Magnitudes of interbar voltages, interbar fault power, and circulating bar currents were all substantially lower for the Z-bar sidewalls. The potentials for arc breakdown at the anode/sidewall corner joints were also reduced in this type of sidewall design. The sidebars were found to align very closely with the direction of plasma equipotential planes, which resulted in the decreased electrical stresses.

The influence of cathode voltage nonuniformities on the electrical properties of segmented-bar sidewalls was also investigated. By the comparison of sidewalls of the same design, the effects of the cathode nonuniformities can be attenuated over shorter distances through greater segmentation of the cathode sidebars. Comparing differing segmented-bar sidewall designs, the interbar voltages on Z-bar sidewalls were lower and more evenly distributed.

The Z-bar insulator wall design was used in a recent coal-fired prototypic MHD generator channel. The sidewall selection was based, in part, on the results of the present study. This generator was part of an integrated topping cycle power train that was used for proof-of-concept testing at a government test facility in Montana. Duration testing was performed at conditions representative of commercial MHD power plant operation to establish component lifetimes and to verify the design performance parameters. The Z-bar sidewalls were in excellent condition after over 500 h of duration testing. Posttest wear measurements suggested the sidewalls can easily exceed the 2000-h lifetime requirement. Furthermore, reliability of the Z-bar design was demonstrated by its trouble-free service throughout the test series.

Acknowledgments

This work was sponsored by the U.S. Department of Energy under Contract DE-AC22-87PC90274 and was funded through TRW, Inc., under Subcontract CX5136D58S. The authors thank L. C. Farrar, D. J. Morrison, and E. W. Schmitt for their assistance in this project.

References

[1]Pian, C. C. P., and Kessler, R., "Open-Cycle Magnetohydrodynamic Power Generators," *Journal of Propulsion and Power*, Vol. 15, No. 2, 1999, pp. 195–203.

[2]Farrar, L. C., "Coal-Fired $1A_1$ Channel Gas-Side Element Design and Materials Test Results from CDIF," *Proceedings of the 28th Symposium on the Engineering Aspects of MHD*, Argonne National Lab., Argonne, IL, 1990, pp. VI.3.1–VI.3.13.

[3]Pian, C. C. P., Petty, S. W., Schmitt, E. W., Morrison, D. J., and Farrar, L. C., "Electrical Characteristics of MHD Generator Sidewalls with Straight- and Z-Bar Designs," *Proceedings of the 29th Symposium on the Engineering Aspects of MHD*, Diagnostic Instrumentation and Analysis Lab., Mississippi State Univ., Mississippi State, MS, 1991, pp. II.2.1–II.2.10.

[4]Pian, C. C. P., and Petty, S. W., "Prototypic MHD Generator Design of the Integrated Topping Cycle Power Train," *Magnetohydrodynamics (MHD) Power Generation, 1991*, edited by N. R. Johanson and J. N. Chapman, AES-Vol. 23, American Society of Mechanical Engineers, New York, 1991, pp. 19–27.

[5]Demirjian, A. M., and Quijano, I. M., "Power Conditioning and Control of Slagging MHD Generators," *Journal of Energy*, Vol. 6, No. 3, 1982, pp. 204–209.

[6]Koester, J. K., and Eustis, R. H., "Coal Slag Phenomena in MHD Generators," Final Rept. Electric Power Research Institute Research Project 46B-1, High Temperature Gasdynamics Lab., Stanford Univ., Stanford, CA, 1982.